

Synthesis of 5-substituted 1*H*-tetrazoles using Cu-doped indium oxide- molecular docking, ADME/pharmacokinetics, biological study

^{1*}Yogeshwar R. Baste, ²Jagdish N. Ghotekar

Research Centre M. V. P. Samaj K. S. K. W. Arts, Science and Commerce College CIDCO, Nashik, Maharashtra, India. Affiliated to Savitribai Phule Pune University Pune

*Corresponding author- *Yogeshwar R. Baste*

Abstract- In this present work, efficient route has been developed for the synthesis of 5-substituted 1*H*-tetrazole derivatives using one pot synthesis using aryl aldehydes (1), sodium azide (2), and hydroxylamine hydrochloride (3) using copper-doped indium oxide (Cu–In₂O₃) nanoparticles as a heterogeneous catalyst. The nano catalyst was synthesized by a hydrothermal method and characterized by XRD, FTIR, SEM-EDS, UV-DRS, and BET analysis, confirming successful copper doping and enhanced surface area. The catalytic system demonstrated excellent activity under mild, environmentally friendly conditions, gives tetrazole derivatives in high purity and yield. The synthesized compounds were evaluated for their potential biological activity, showing promising antimicrobial properties. In silico ADME profiling using Swiss-ADME indicated favourable drug-like properties, including good gastrointestinal absorption and compliance with Lipinski's rule of five. Furthermore, molecular docking studies revealed strong binding interactions of the tetrazole derivatives with selected biological targets, supporting their potential as lead compounds for pharmaceutical development. The use of this method offers advantages for the synthesis of 5-substituted 1*H*-tetrazole derivatives, includes easily available starting precursors, simple and ease operate, highly pure product obtained with good yields.

Keywords 5-substituted 1*H*-tetrazole, Hydrothermal method, Swiss-ADME, Molecular docking.

INTRODUCTION

Heterocyclic compounds are found to be biologically active, hence having quite large interest in chemistry. These compounds can be synthesized using various routes. Among them, tetrazole derivatives as a nitrogen-rich five-membered ring are the important class of heterocyclic compounds [1-3]. Tetrazole

derivatives, particularly 5-substituted 1*H*-tetrazoles, have garnered significant attention due to their broad spectrum of applications in pharmaceuticals, agrochemicals, and materials science [4]. Traditional methods for synthesizing 5-substituted tetrazoles typically involve [3+2] cycloaddition reactions between organic nitriles and sodium azide, often requiring harsh conditions or toxic solvents [5-7]. To address these challenges, recent studies have emphasized the creation of sustainable and highly effective catalytic systems [8-12]. To overcome and minimize this difficulty, metal oxide nanoparticles are used as efficient catalysts because of a large surface area, are easy to recover, and can be used multiple times. Among them, copper-doped indium oxide (Cu–In₂O₃) nanoparticles have gained attention for their enhanced catalytic performance, attributed to synergistic effects between copper and indium species, improved electron transfer properties, and increased active surface sites [13-15]. The hydrothermal synthesis of these nano catalysts offers a controllable and scalable route to obtain uniform particles with desirable physicochemical characteristics. Their application in the synthesis of tetrazole derivatives not only improves reaction efficiency under milder and greener conditions but also aligns well with the principles of sustainable chemistry. In recent years, the development of heterogeneous catalytic systems has emerged as a promising strategy to improve the efficiency, sustainability, and reusability of these transformations.

Herein, we try to report a simple and useful procedure for the synthesis of 5-substituted 1*H*-tetrazole derivatives via a one-pot three-component reaction of

aryl aldehyde, sodium azide, and hydroxylamine hydrochloride using hydrothermally synthesized Cu-doped indium oxide as a stable and recyclable catalyst.

II RESULTS AND DISCUSSIONS

Synthesis and characterization of nano-catalyst

The Cu-doped indium oxide was synthesized at the nano level and in highly pure form by the use of the hydrothermal method, and after complete synthesis, the oxide was characterized by several investigating methods involving UV-DRS for the band gap study, FTIR for the functional group determination, XRD for the particle size determination, BET for the surface area analysis, and SEM-EDS for the investigation of surface morphology and elemental compositions.

UV-visible absorption spectra clearly indicate that the Cu-doped indium oxide shows absorption maxima (λ_{max}) at 294 nm (Figure 2) has a band gap of 4.22 eV, which is calculated from the formula $1240/\lambda_{\text{max}}$.

FTIR peaks (Figure 3) at 601 to 420 cm^{-1} to the formation of Cu-doped In-O frequency [16].

The XRD study of hydrothermally synthesized Cu-doped indium oxide shows an orthorhombic system that is closely matched with the Cu-doped indium oxide (JCPDS Card No. 73-1592). Using the data available from the XRD analysis, the obtained peaks at 2θ values, 21.3038, 30.8242, 35.8354, 51.3701, and 60.9916 correspond to the planes 600, 530, 611, 1230, and 1141, respectively. The average particle size for Cu-doped indium oxide was calculated from the Scherrer formula ($D = K\lambda / \beta \cos\theta$), and ImageJ software was found to be 16.59 and 16.31 nm, respectively, as shown in Figures 4 and 5.

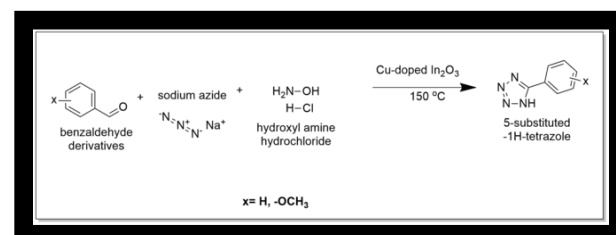
The surface morphology of Cu-doped indium oxide was investigated by using FE-SEM technique. This study indicates that the hydrothermally synthesized Cu-doped indium oxide forms with an average particle size of 16.31 nm (Figure 6). The elemental analysis confirms the stoichiometric amount taken for the synthesis, as shown in Figures 7 to 9.

The hydrothermal synthesis method gives Cu-doped indium oxide particles at the nanoscale; the surface area was investigated by using the BET surface area method. The pore volume, mean pore diameter, and

surface area for Cu-doped indium oxide were found to be $0.2488 \text{ cm}^3 \text{ g}^{-1}$, 54.169 nm, and $18.372 \text{ m}^2 \text{ g}^{-1}$, respectively (Figure 10).

Synthesis towards various 5-substituted 1H-tetrazole derivatives

We planned to synthesis of 5-substituted 1H-tetrazole and its derivatives, by taking consideration of their amazing properties. For this purpose, we utilized Cu-doped indium oxide as a heterogeneous catalyst. The one-pot multicomponent reaction of aryl aldehydes, sodium azide, and hydroxylamine hydrochloride to form the desired 5-substituted 1H-tetrazole derivatives was achieved in an efficient manner. In this context, in order to achieve optimum reaction conditions, various parameters like temperature, solvent, amount of catalyst, and reaction time were optimized. Initially, aryl aldehyde (1 mmol), sodium azide (1 mmol), and hydroxylamine hydrochloride (1 mmol) underwent a one-pot reaction under various conditions. Later, under similar reaction conditions, the effect of the solvent has been determined for different solvents like water, ethanol, methanol, toluene, DMF, and DCM, as illustrated in Table number 6. Ethanol was found to be the best solvent with the shortest reaction time and maximum yield at 150°C in the presence of Cu-doped indium oxide. The optimum dose of catalyst reaction was performed by utilizing various amounts of catalyst (1, 3, 5, 7, and 10 mol %) using ethanol as a solvent at 150°C . From Table 1, it can be concluded that 3 mol % of catalyst dose is sufficient for this reaction to obtain maximum yield at 150°C using ethanol as a solvent. The obtained products were purified without the use of chromatographic techniques; however, recrystallization using ethanol gives pure compounds. At these optimized reaction conditions, we performed reactions using various aryl aldehydes with sodium azide and hydroxylamine hydrochloride to obtain corresponding derivatives of 5-substituted 1H-tetrazole. The overall general reaction is summarized in Scheme 1, and melting points and reaction time are summarized in Table 2.



Scheme 1: Synthesis of 5-substituted 1*H*-tetrazole derivatives using Cu-doped indium oxide.

The characterization of tetrazole derivatives was carried out using multiple analytical techniques, including FTIR, ¹H NMR, ¹³C NMR, and high-resolution mass spectrometry (HRMS).

The reusability and recycling tendency of synthesized Cu-doped indium oxide were tested at the optimum conditions of the reaction. A simple method can be adopted for the recovery of the catalyst. After completion of the reaction, the catalyst was simply recovered, washed with water and ethanol, and dried under vacuum with low heat to remove any attached impurities. After that, it can be reused again. From Figure 1, it can be clearly observed that the synthesized nano catalyst can be used more than two times without any significant decrease in catalytic performance.

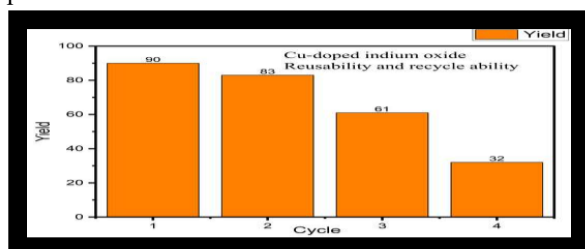


Figure 1: Reusability of Cu-doped indium oxide catalyst.

Antimicrobial study of Cu-doped indium oxide and 5-substituted 1*H*-tetrazole derivatives

The antimicrobial potential of the synthesized Cu-doped indium oxide and 5-substituted 1*H*-tetrazole derivatives was evaluated against a panel of pathogenic microorganisms, including *Escherichia coli*, *Pseudomonas aeruginosa*, *Staphylococcus aureus*, and *Candida albicans*. The antimicrobial activities of these derivatives were assessed by measuring the diameters of the inhibition zones in millimetres. Several of the tetrazole derivatives exhibited significant antibacterial activity, particularly against *S. aureus* and *E. coli*, while moderate antifungal effects were observed against *C. albicans* illustrated in Table 3. These findings suggest that tetrazole-based molecules may offer promising scaffolds for developing new antimicrobial agents.

Swiss-ADMET/Pharmacokinetics study of 5-substituted 1*H*-tetrazole derivatives

The pharmacokinetic properties and drug-likeness of the synthesized 5-substituted 1*H*-tetrazole derivatives were assessed using the Swiss-ADME online tool. Key parameters such as absorption, distribution, metabolism, and excretion (ADME) were predicted to evaluate the potential of these compounds as oral drug candidates. All compounds were found to comply with Lipinski's rule of five, indicating favourable oral bioavailability. The predicted high gastrointestinal (GI) absorption and good blood-brain barrier (BBB) permeability of selected derivatives suggest their potential for systemic therapeutic use. In addition, none of the compounds showed inhibition of key cytochrome P450 isoforms, implying a lower likelihood of drug-drug interactions. The bioavailability radar and BOILED-Egg models further supported the favorable pharmacokinetic profile of the compounds, highlighting their balance between lipophilicity and polarity. Overall, the Swiss-ADME analysis suggests that the 5-substituted tetrazole derivatives possess promising drug-like characteristics, making them suitable candidates for further biological evaluation illustrated in Figures 4 to 14 and illustrated in Table 4.

Molecular Docking

To gain insight into the potential mechanism of antimicrobial activity, molecular docking studies were performed for the synthesized 5-substituted 1*H*-tetrazole derivatives against selected protein targets from *Escherichia coli*, *Pseudomonas aeruginosa*, *Staphylococcus aureus*, and *Candida albicans*. The crystal structures of essential microbial enzymes, such as DNA gyrase (*E. coli*, PDB ID: 1KZN), LasR quorum sensing regulator (*P. aeruginosa*, PDB ID: 2UV0), dihydrofolate reductase (*S. aureus*, PDB ID: 2W9H), and lanosterol 14 α -demethylase (*C. albicans*, PDB ID: 5TZ1), illustrated in Table 5 and were retrieved from the Protein Data Bank and prepared using standard molecular docking protocols. Docking simulations were carried out using AutoDock or similar tools to evaluate the binding affinity and interaction profiles of the compounds. Several derivatives demonstrated strong binding energies and stable interactions within the active sites, primarily through hydrogen bonding, π - π stacking, and hydrophobic interactions. These findings correlate well with the *in vitro* antimicrobial results and suggest that tetrazole derivatives may inhibit vital microbial

pathways by effectively interacting with target proteins, supporting their potential as broad-spectrum antimicrobial agents. Figures 15-26.

Experimental Section

For the synthesis of Cu-doped indium oxide and tetrazole derivatives, all the required chemicals and reagents were purchased from SRL (99.9% pure) and Sigma Aldrich and were used without any further purification. The nanocatalyst was characterized by FTIR (FT/IR-4600 type A), FE-SEM (FEI Nova Nano SEM 450), EDS (Bruker X Flash 6130), XRD (Bruker, D8 Discover, powder XRD Cu K α λ 1.5406 Å), UV-DRS (V770, Jasco, Japan), and BET surface area. The synthesized tetrazole derivatives were characterized by ¹H-NMR and ¹³C-NMR (Bruker Avance III HD NMR 500 MHz) in DMSO. The FTIR and HRMS analysis was done by dlc_50-120mz, pos_mode_7min_0.2mlm. The source used ESI type (Bruker Impact HD). The progress of the reaction was checked on TLC using ethyl acetate and n-hexane, and melting points were determined by the open capillary method and were uncorrected.

Catalyst Synthesis

After optimization of reaction conditions, Cu-doped indium oxide was synthesized by the hydrothermal method using a stainless-steel, Teflon bottle autoclave using indium nitrate (99.9% pure SRL) and copper nitrate (99.9% pure SRL) as precursors and 1 M NaOH as a precipitating agent. The autoclave is heated in a hot air oven at 170°C for 8 hours and was cooled at RT. The precipitate was collected, washed using water, and calcinated at 650°C in a muffle furnace until complete conversion into oxide. The synthesized material was investigated by FTIR, UV-DRS, XRD, SEM-EDS, and BET surface area analysis.

General method for synthesis of 5-substituted 1H-tetrazole derivatives

For the synthesis of 5-substituted 1H-tetrazole derivatives, aryl aldehyde (1 mmol), sodium azide (1 mmol), hydroxylamine hydrochloride (1 mmol), and a catalyst were added, and the RB flask was placed in an oil bath where the temperature was maintained at 160°C. The progress of the reaction was checked by TLC, and after confirming product was formed, the reaction mixture was cooled at RT, the catalyst was recovered, and the mixture was poured into crushed

ice. Filter, wash, and dry the product to find yield. The product was recrystallized using pure alcohol. The synthesized derivatives were characterized by NMR, FTIR, and HRMS. The results of characterization, yield, and melting point of derivatives were recorded.

4A) 5-phenyl-1H-tetrazole

Pure product (white solid, 88-90 % yield, TLC 1:3 Ethyl acetate and n-hexane) melting point- 215-216 °C.

FTIR frequency at 3150, 3078, 3055, 3001, 2401, 1610, 1479, 1465, 1151, 688 cm⁻¹.

¹H NMR (500 MHz, DMSO) δ ppm: 8.06 (s, 1H), 7.60-7.60 (s, 1H).

¹³C NMR (500 MHz DMSO) δ ppm 124.78, 127.46, 129.91, 131.66.

HRMS fragmentation (ESI⁺ ion polarity) of C₇H₆N₄ gives an observed molecular weight of [M+H] 147.0671 matches with the theoretical molecular weight of 146.15 grams per mol.

4B) 5-(4-methoxyphenyl)-1H-tetrazole

Pure product (white solid, 85-88 % yield, TLC 1:3 Ethyl acetate and n-hexane) melting point- 114-116 °C.

FTIR frequency at 3450, 3061, 1612, 1500, 1164 cm⁻¹.

¹H NMR (500 MHz, DMSO) δ ppm: 8.44-8.45 (s, 1H), 8.00-8.02 (d, 2H), 7.15-7.17 (d, 2H), 3.99 (s, 3H).

¹³C NMR (500 MHz DMSO) δ ppm 161.90, 129.13, 116.80, 115.31, 55.91.

HRMS fragmentation (ESI⁺ ion polarity) of C₈H₈N₄O gives an observed molecular weight of [M+H] 177.0773 matches with the theoretical molecular weight of 176.18 grams per mol.

Data availability

The data supporting this article have been included.

Conflict of interest

There is no conflict to declare.

V. HELPFUL HINTS

A. Figures and Tables

Characterisation of Cu-doped indium oxide.

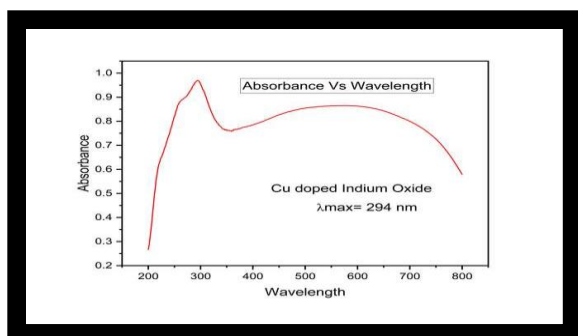


Figure 2: UV-DRS Cu-doped indium oxide.

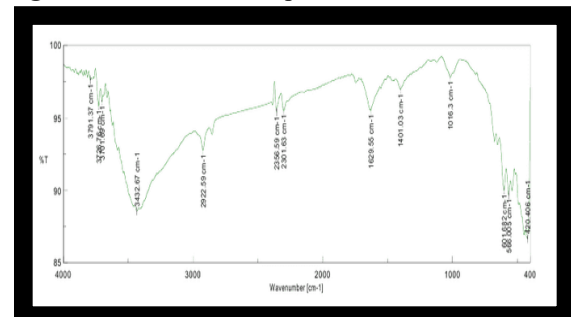


Figure 3: FTIR Cu-doped indium oxide.

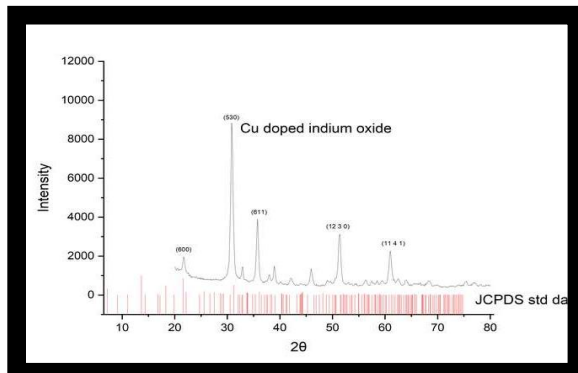


Figure 4: XRD Cu-doped indium oxide.

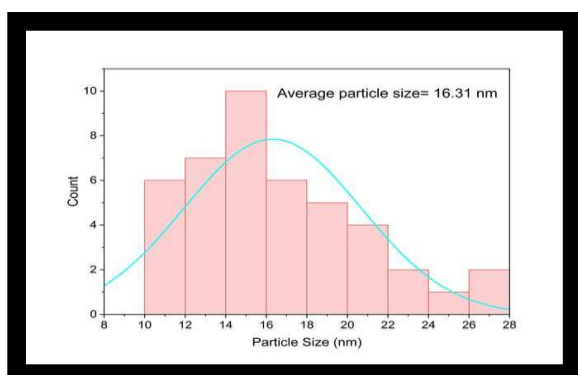


Figure 5: Average size Cu-doped indium oxide.

XRD Cu-doped indium oxide. **Figure 6:** Average size Cu-doped indium oxide.

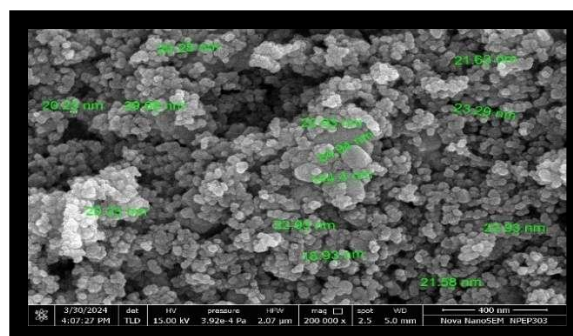


Figure 7: SEM Cu-doped indium oxide.

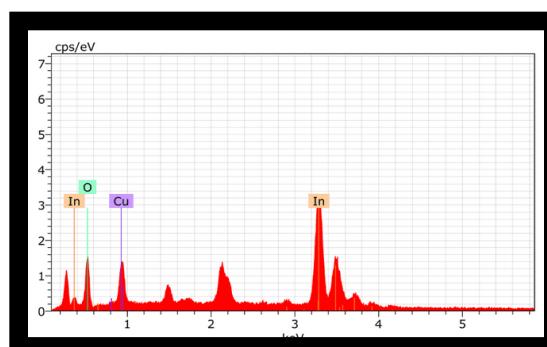


Figure 8: EDS Cu-doped indium oxide.

Savitribai Phule Pune University
Central Instrumentation Facility
EDS Report

Spectrum: OBJECT 117

El	AN	Series	unn.	C norm.	C Atom.	C Error (1 Sigma)
			[wt.%]	[wt.%]	[at.%]	[wt.%]
In	49	L-series	43.47	59.43	23.72	1.37
O	8	K-series	16.04	21.93	62.83	2.62
Cu	29	K-series	13.63	18.64	13.44	0.57
Total:			73.15	100.00	100.00	

Figure 9: Composition Cu-doped indium oxide.

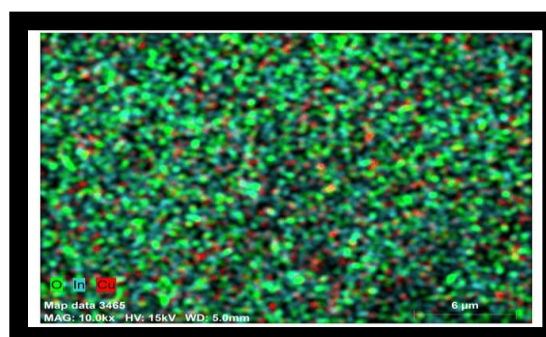


Figure 10: 3D image Cu-doped indium oxide.

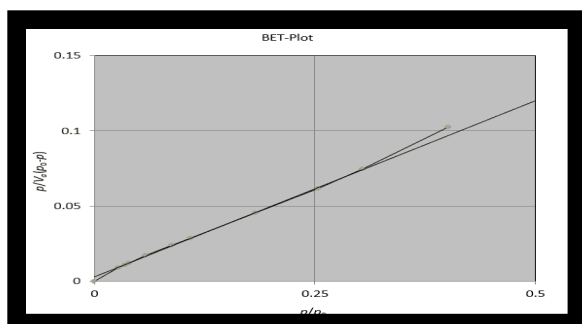


Figure 11: BET Cu-doped indium oxide. Swiss-ADMET/Pharmacokinetics study of synthesized imidazole derivatives (4A and 4B)

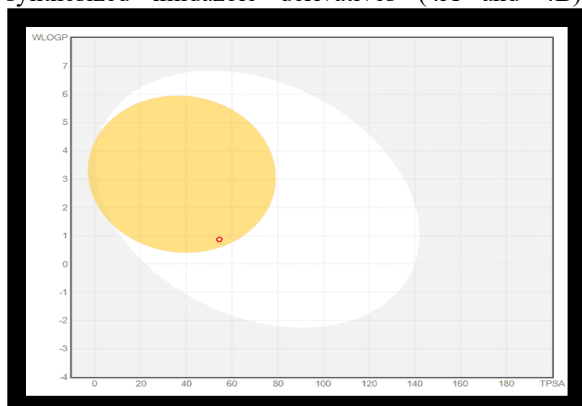


Figure 12: BOILED-Egg model 4A.

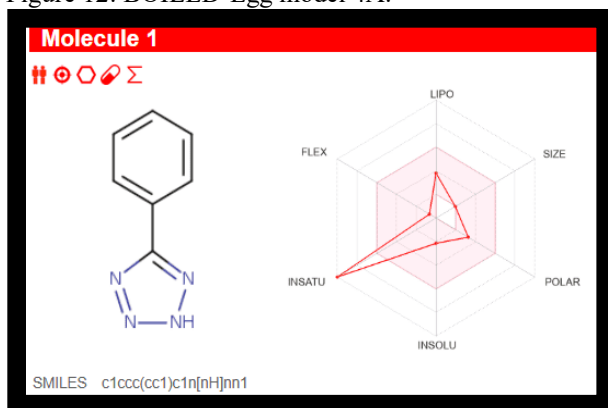


Figure 12: Bioavailability radar 4A.

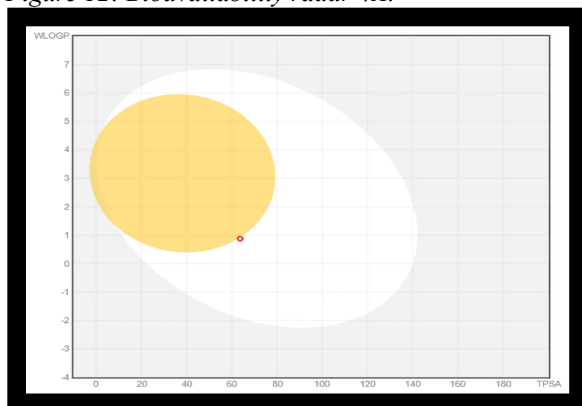


Figure 13: BOILED-Egg model 4B.

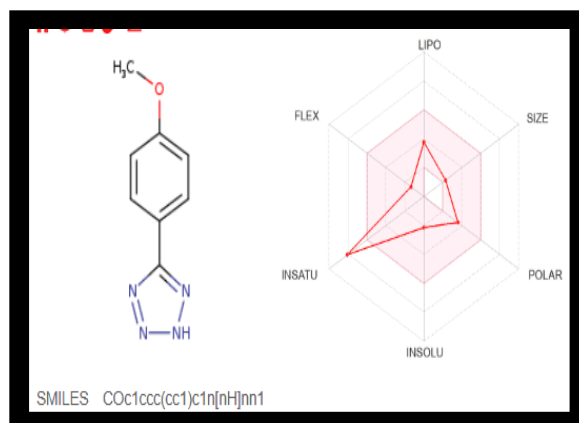


Figure 14: Bioavailability score 4B. Molecular Docking between E. Coli (as a receptor) and 4A (as a ligand).

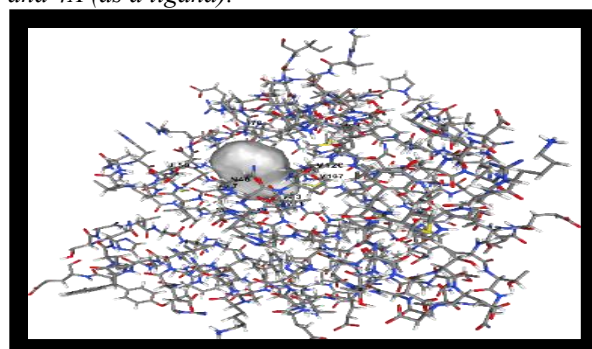


Figure 15: Docking complex E. coli and 4A.

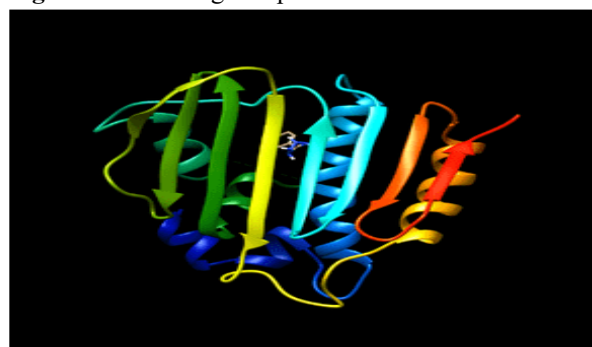


Figure 16: Rainbow structure. Molecular Docking between E. Coli (as a receptor) and 4B (as a ligand).

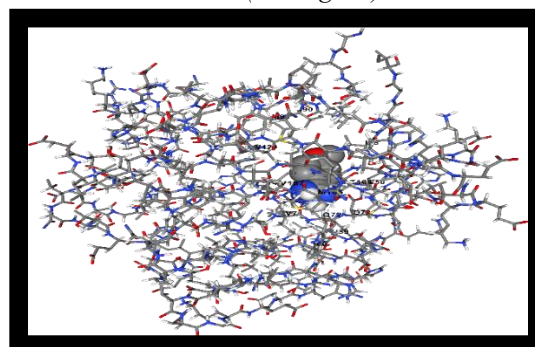


Figure 17: Docking complex E. coli and 4B.

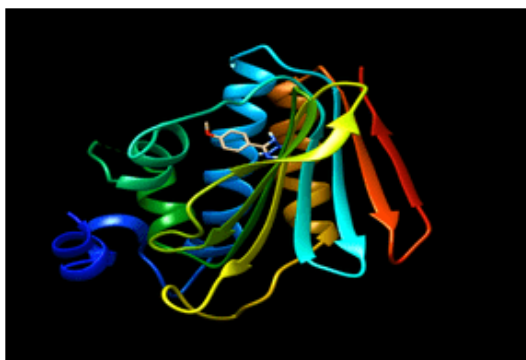


Figure 18: Rainbow structure.
Molecular Docking Between *Staphylococcus aureus*
(as a receptor) and 4A (as a ligand)

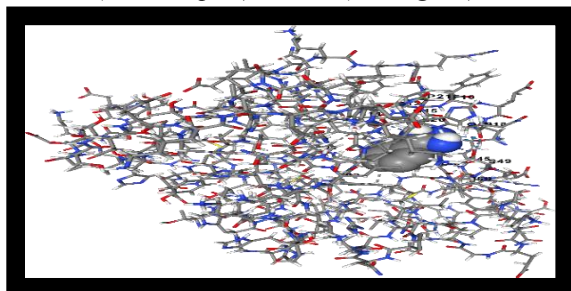


Figure 19: Docking complex.

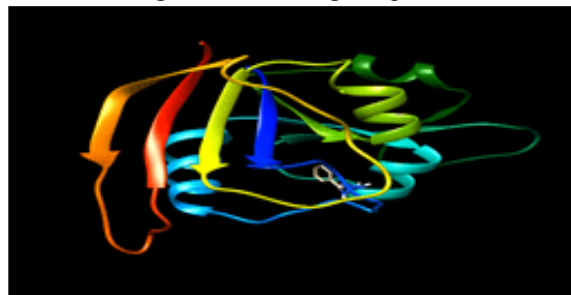


Figure 20: Rainbow structure.
Molecular Docking Between *Staphylococcus aureus*
(as a receptor) and 4B (as a ligand)

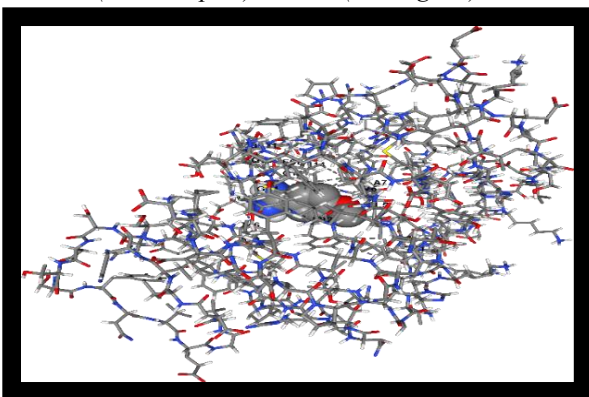


Figure 21: Docking complex.

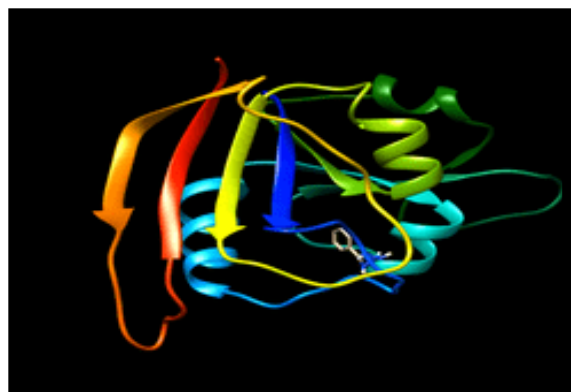


Figure 22: Rainbow structure.
Molecular Docking between *Pseudomonas*
Aeruginosa (as a receptor) and 4A (as a ligand)

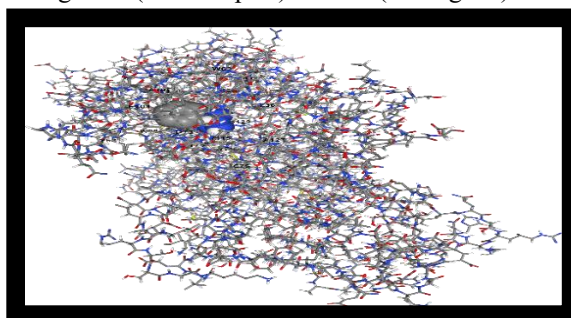


Figure 23: Docking complex.

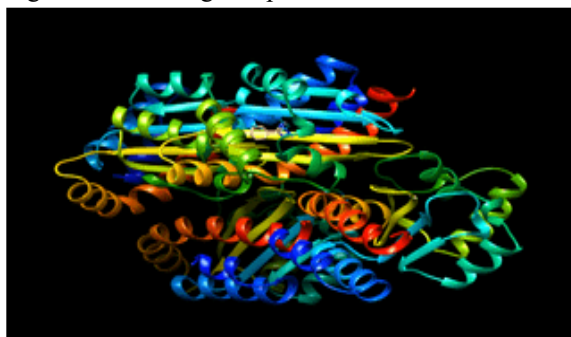


Figure 24: Rainbow structure.
Molecular Docking between *Pseudomonas*
Aeruginosa (as a receptor) and 4B (as a ligand)

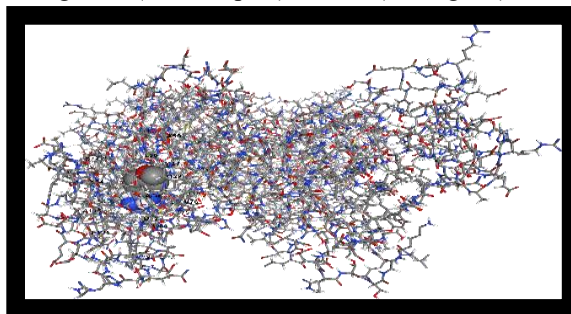


Figure 25: Rainbow structure.



Figure 26: Docking complex.

Table 1: Optimization of reaction parameters for the synthesis of 5-phenyl-1H-tetrazole derivatives.

Entry	Catalyst Amount (mol %)	Time (h)	Temp (°C)	Yield (%)
1	No catalyst	10	RT	0
2	No Catalyst	10	50	0
3	No Catalyst	10	100	Trace
4	1	2.5	80	50
5	3	2	100	90
6	5	2	100	80
7	7	2	100	82
8	10	2	100	81

Table 2: Synthesis of 5-phenyl-1H-tetrazole derivatives (4A-4B) using Cu-doped indium oxide.

Sr. No.	Aldehyde	Catalyst	Yield %	R.T (min)	M.P. °C	M.F	M. wt. g/mol
1 A	C ₆ H ₅ -	Cu-doped In ₂ O ₃	90	100	271-272	C ₇ H ₆ N ₄	146.15
1 C	4-OCH ₃ C ₆ H ₅	Cu-doped In ₂ O ₃	88	100	114-116	C ₈ H ₈ N ₄ O	176.18

Table 3: Antimicrobial Activities of 5-phenyl-1H-tetrazole derivatives (4A-4C).

Sr. No.	Compound	Antimicrobial			Antifungal
		<i>E. Coli</i>	<i>Pseudomonas aeruginosa</i>	<i>Staphylococcus aureus</i>	
		ATCC 25922	ATCC 27853	ATCC 25923	ATCC 14053

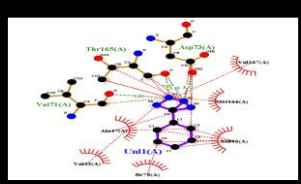
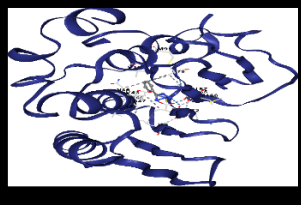
1.	5-phenyl-1H-tetrazole (4A)	7 mm	5 mm	8 mm	6 mm
2.	5-(4-methoxyphenyl)-1H-tetrazole	9 mm	7 mm	10 mm	8 mm
3.	Cu-doped indium oxide	7 mm	7 mm	No zone	No zone
4.	Gentamicin	23 mm	24 mm	26 mm	-

Table 4: Swiss-ADME prediction results for synthesized 5-phenyl-1H-tetrazole derivatives (4A-4B).

Sr. No	Parameter	4A	4B
1	Lipinski's Rule (drug-likeness)	Obeyed (0 violations)	Obeyed (0 violation)
2	GI Absorption	High	High
3	BBB Permeability	Yes	No
4	P-gp Substrate	No	No
5	CYP1A2 Inhibitor	No	No
6	CYP3A4 Inhibitor	No	No
7	Bioavailability Score	0.85	0.85
8	Water Solubility	Soluble	Soluble
9	BOILED-Egg Result	BBB & HIA zone (Figure 12)	HIA zone (Figure 13)
10	Log K _p (Skin Permeation)	-6.38 cm/s	-6.59 cm/s
11	TPSA	54.46	63.69

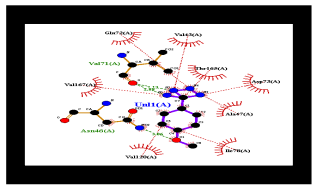
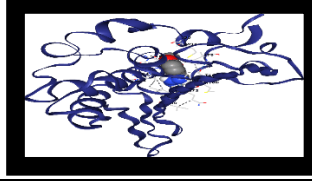
Table 5: Molecular Docking results of synthesized 5-phenyl-1H-tetrazole derivatives (4A and 4B) with [Target Protein *E. Coli*, *Pseudomonas Aeruginosa*, *Staphylococcus Aureus*].

Sr. No.	Parameter	Description
A) Molecular Docking between <i>E. Coli</i> and 4A.		
1	Ligand name	5-phenyl-1H-tetrazole
2	Protein Target	Thymidylate synthase from <i>Escherichia coli</i> PDB ID: 1KZN
3	Binding Energy (kcal/mol)	-6.6
4	Inhibition Constant (ki)	14.5 μM (micromolar)
5	Docking Software	CB Dock 2
6		Grid Size 17 X 25 X 17 Å ⁰

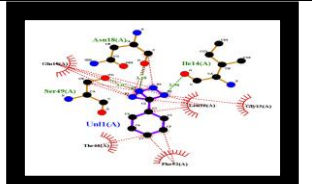
	Grid Parameters	Spacing Centre coordinates	1 Å ⁰ 20, 23, 35
7	Number of docking poses	9 and best docking pocket C ₄	
8	Interacting amino acids	Chain A: GLU42 VAL43 VAL44 ASN46 ALA47 ILE48 ASP49 GLU50 ILE59 VAL71 GLN72 ASP73 GLY75 ARG76 GLY77 ILE78 PRO79 VAL89 ILE90 MET91 VAL93 LEU94 HIS95 ALA96 GLY117 VAL118 GLY119 VAL120 SER121 VAL122 ARG136 GLY164 THR165 MET166 VAL167	
9	Type of interaction		
10	Ligand Confirmations (Docking Complex)		
11	Visualization tool	Protein-Ligand Interaction Profiler.	


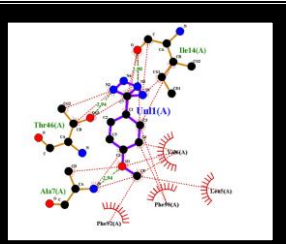
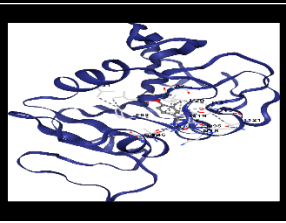
B) Molecular Docking between E. Coli and 4B.

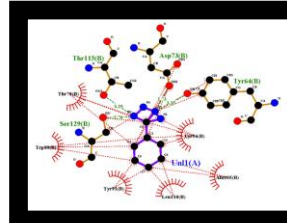
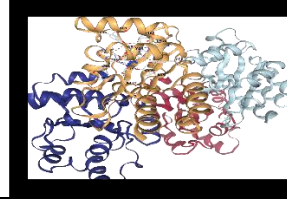
1	Ligand name	5-(4-methoxyphenyl)-1H-tetrazole	
2	Protein Target	Thymidylate synthase from Escherichia coli PDB ID: 1KZN	
3	Binding Energy (kcal/mol)	-7.0	
4	Inhibition Constant (ki)	7.5 micromolar (µM).	
5	Docking Software	CB Dock 2	
6	Grid Parameters	Grid Size	18 X 25 X 18 Å ⁰
		Spacing	1 Å ⁰
		Centre coordinates	20, 23, 35
7	Number of docking poses	9 and best docking pocket C ₁	
8	Interacting amino acids	Chain A: GLU42 VAL43 VAL44 ASP45 ASN46 ALA47 ASP49 GLU50 ILE59 VAL71 GLN72 ASP73 ARG76 GLY77 ILE78 PRO79 VAL89 ILE90 MET91 THR92 VAL93 LEU94 HIS95 ALA96 GLY117 VAL118	

		GLY119 VAL120 SER121 VAL122 ARG136 THR165 MET166 VAL167
9	Type of interaction	
10	Ligand Confirmations (Docking Complex)	
11	Visualization tool	Protein-Ligand Interaction Profiler.

C) Molecular Docking between S. Aureus and 4A.

1	Ligand name	5-phenyl-1H-tetrazole	
2	Protein Target	Staphylococcus aureus DHFR incomplex with trimethoprim. PDB ID: 2W9H.	
3	Binding Energy (kcal/mol)	-6.2	
4	Inhibition Constant (ki)	28.6 micromolar (µM).	
5	Docking Software	CB Dock 2	
6	Grid Parameters	Grid Size	23 X 23 X 24
		Spacing	1 Å ⁰
		Centre coordinates	14, -4, 18
7	Number of docking poses	9 and best docking pocket C ₁ .	
8	Interacting amino acids	Chain A: LEU5 VAL6 ALA7 HIS8 ILE14 GLY15 PHE16 ASN18 GLN19 LEU20 PRO21 TRP22 PRO25 ASP27 LEU28 LYS29 VAL31 LYS32 MET42 GLY43 ARG44 LYS45 THR46 SER49 ILE50 LEU54 ARG57 PHE92 GLY93 GLY94 GLN95 THR96 LEU97 PHE98 THR111 THR121	
9	Type of interaction		

10	Ligand Confirmations (Docking Complex)		
11	Visualization tool	Protein-Ligand Interaction Profiler.	
D) Molecular Docking between S. Aureus and 4B.			
1	Ligand name	5-(4-methoxyphenyl)-1H-tetrazole	
2	Protein Target	Staphylococcus aureus DHFR incomplex with trimethoprim. PDB ID: 2W9H.	
3	Binding Energy (kcal/mol)	-6.5	
4	Inhibition Constant (ki)	17.1 micro molar (μM)	
5	Docking Software	CB Dock 2.	
6	Grid Parameters	Grid Size	18 X 18 X 24
		Spacing	1 Å ⁰
		Centre coordinates	14, -4, 18
7	Number of docking poses	9 and best docking pocket C ₁ .	
8	Interacting amino acids	Chain A: LEU5 VAL6 ALA7 ILE14 GLY15 ASN18 GLN19 LEU20 TRP22 ASP27 LEU28 VAL31 GLY43 LYS45 THR46 SER49 ILE50 PHE92 GLY93 GLY94 GLN95 THR96 LEU97 PHE98 ASP120 THR121.	
9	Type of interaction		
10	Ligand Confirmations (Docking Complex)		
11	Visualization tool	Protein-LigandInteraction Profiler.	
E) Molecular Docking between P. aeruginosa and 4A.			
1	Ligand name	5-phenyl-1H-tetrazole	
2	Protein Target	Pseudomonas Aeruginosa PDB ID: 2UV0	

3	Binding Energy (kcal/mol)	-8.7	
4	Inhibition Constant (ki)	0.426 micromolar (μM)	
5	Docking Software	CB Dock 2.	
6	Grid Parameters	Grid Size	17 X 17 X 17
		Spacing	1 Å ⁰
		Centre coordinates	55, 29, 29
7	Number of docking poses	9 and best docking pocket C ₃ .	
8	Interacting amino acids	Chain B: LEU36 GLY38 LEU39 LEU40 ASP46 TYR47 GLU48 ALA50 PHE51 ILE52 TYR56 TRP60 ARG61 TYR64 ASP65 ALA70 ASP73 THR75 VAL76 CYS79 TRP88 TYR93 PHE101 ALA105 LEU110 LEU114 THR115 LEU125 GLY126 ALA127 SER129	
9	Type of interaction		
10	Ligand Confirmations (Docking Complex)		
11	Visualization tool	Protein-LigandInteraction Profiler.	
F) Molecular Docking between P. aeruginosa and 4B.			
1	Ligand name	5-(4-methoxyphenyl)-1H-tetrazole	
2	Protein Target	Pseudomonas Aeruginosa PDB ID: 2UV0	
3	Binding Energy (kcal/mol)	-8.1	
4	Inhibition Constant (ki)	1.16 micro molar (μM)	
5	Docking Software	CB Dock 2.	
6	Grid Parameters	Grid Size	18 X 18 X 18
		Spacing	1 Å ⁰
		Centre coordinates	55, 29, 29
7	Number of docking poses	9 and best docking pocket C ₃ .	

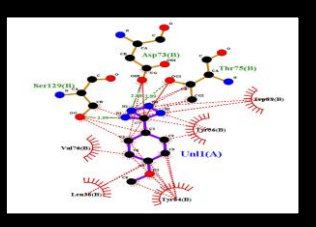
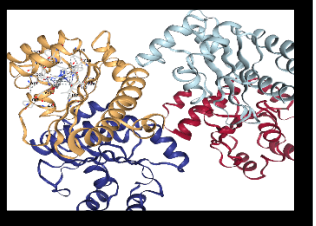
8	Interacting amino acids	Chain B: LEU36 GLY38 LEU39 LEU40 ASP46 TYR47 GLU48 ALA50 ILE52 TYR56 TRP60 ARG61 TYR64 ASP65 ALA70 ASP73 THR75 VAL76 TRP88 TYR93 PHE101 LEU110 LEU114 THR115 GLY126 ALA127 SER129
9	Type of interaction	
10	Ligand Confirmations (Docking Complex)	
11	Visualization tool	Protein-Ligand Interaction Profiler.

Table 6: Effect of solvent on the 5-phenyl-1H-tetrazole derivative using 3 mol % Cu-doped indium oxide catalyst.

Sr. No.	Solvent	Time (min)	Yield (%)
1	Water	120	No reaction
2	Methanol	110	60
3	Toluene	140	40
4	DMF	130	80
5	DCM	150	52
6	Ethanol	100	90

CONCLUSION

An effective and convenient one-pot three-component strategy has been developed for the synthesis of 5-substituted 1H-tetrazole derivatives using nanosized Cu-doped indium oxide as a catalyst. The Cu-doped indium oxide nano catalyst was synthesized in highly pure form by the use of the hydrothermal method. The synthesized tetrazole derivatives need no further purification by the chromatographic techniques; they can be obtained in pure form only by simple recrystallization using ethanol, which is the precious advantage of this work. These results confirm the effective catalytic performance of Cu-doped indium oxide. These tetrazole derivatives show positive antimicrobial activities; hence, an excellent docking

score is obtained in the molecular docking. Along with this, Swiss-ADMET focused on pharmacokinetics and bioavailability of synthesized 5-substituted 1H-tetrazole derivatives.

ACKNOWLEDGMENT

The authors are very thankful to CIF, S P University Pune, and DST FIST Jaysingpur for cooperation. The authors extend their sincere gratitude to Prof. (Dr.) S. K. Kushare, Principal, MVP Samaj's KSKW Arts, Science and Commerce College, CIDCO, Nashik, for his valuable guidance and constant support throughout this work. The authors would like to express heartfelt thanks to Mr. Pratik Bhabad, Mr. Krushna Khule, Mr. Aniket Gurav, and Ms. Sonali Jadhav for their kind cooperation

REFERENCE

- [1] J. L. Stymiest, V. Bagutski, R. M. French and V. K. Aggarwal, *Nature*, 2008, 456, 778–782.
- [2] A. A. Sabnis, *Synth. Commun.*, 2003, 33, 429–435.
- [3] J. H. Chong, M. J. MacLachlan and D. G. Hall, *Tetrahedron Lett.*, 2003, 44, 8677–8681.
- [4] P. Demko and K. Sharpless, *J. Org. Chem.*, 2001, 66, 7945–7950.
- [5] Y. G. Manohar, S. D. Sharma and D. Konwar, *Tetrahedron Lett.*, 2008, 49, 2216–2220.
- [6] G. W. Kabalka, R. R. Wadgaonkar and M. M. Malladi, *Synth. Commun.*, 1993, 23, 1643–1648.
- [7] B. Karthikeyan, A. Pandurangan and R. A. Kumar, *J. Mol. Catal. A: Chem.*, 2015, 410, 14–23.
- [8] A. M. Ghorab, H. M. Refat, A. E. Amr and M. M. Abdel-Aziz, *Eur. J. Med. Chem.*, 2011, 46, 5675–5681.
- [9] S. N. Azizi, F. Momeni and R. Heydari, *Appl. Organomet. Chem.*, 2020, 34, e5633.
- [10] H. Eshghi, Z. Khashyarmansh and S. Rostamnia, *RSC Adv.*, 2015, 5, 93979–93987.
- [11] M. Darroudi, M. Rezaei and S. Amrollahi, *RSC Adv.*, 2016, 6, 40976–40984.
- [12] S. Chen, B. Mulgrew, and P. M. Grant – A clustering technique for digital communications channel equalization using radial basis function networks, *IEEE Trans. On Neural Networks*, vol. 4, pp. 570– 578, July 1993.
- [13] J. U. Duncombe, –Infrared navigation—Part I : An assessment off feasibility, *IEEE Trans.*

- Electron Devices*, vol. ED-11, pp. 34-39, Jan. 1959.
- [14] C.Y. Lin, M. Wu, J.A. Bloom, I. J. Cox, and M. Miller, –Rotation, scale, and translation resilient public watermarking for images, | *IEEE Trans. Image Process.*, vol. 10, no, pp. 767-782, May 2001. Springer-Verlag, 1985, ch. 4.
 - [15] Guggilapu, S. D.; Prajapati, S. K.; Nagarsenkar, A.; Gupta, K. K.; Babu, B. N. Synlett 2016, 27, 1241–1244.
 - [16] Chu, D. W.; Zeng, Y.-P.; Jiang, D. Appl. Phys. Lett. 2008, 92, 182110.
 - [17] Sivakumar, N.; Ananthalakshmi, S.; Ruso, J. S. J. Adv. Sci. Res. 2019, 10(03 Suppl 1), 247–251.
 - [18] Mitra, B.; Mukherjee, S.; Pariyar, G. C.; Ghosh, P. Tetrahedron Lett. 2018, 59, 1385–1389.
 - [19] Al-Agel, F. A.; Al-Arfaj, E.; Al-Ghamdi, A. A.; Losovyj, Y.; Bronstein, L. M.; Mahmoud, W. E. J. Magn. Magn. Mater. 2014, 360, 73–79.
 - [20] Zhu, P.; Wu, W.; Zhou, J.; Zhang, W. Appl. Organomet. Chem. 2007, 21, 909–912.
 - [21] Yang, H.; Tang, A.; Zhang, X.; Yang, W.; Qiu, G. Scr. Mater. 2004, 50, 413–415.
 - [22] Combe, E.; Chubilleau, C.; Berardan, D.; Guilmeau, E.; Maignan, A.; Raveau, B. Powder Technol. 2011, 208, 503–508.
 - [23] Prakash, R.; Kumar, S.; Ahmed, F.; Lee, C. G.; Song, J. I. Thin Solid Films 2011, 519, 8243–8246.
 - [24] Naik, M. Z.; Salker, A. V. Mater. Res. Innov. 2017, 21, 237–243.
 - [25] Ye, F.; Cai, X. M.; Zhong, X.; Tian, X. Q.; Jing, S. Y.; Huang, L. B.; Roy, V. A.; Zhang, D. P.; Fan, P.; Luo, J. T.; Zheng, Z. H. Thin Solid Films 2014, 556, 44–47.
 - [26] Oh, J. H.; Seong, T. Y.; Hong, H. G.; Kim, K. K.; Yoon, S. W.; Ahn, J. P. J. Electroceram. 2011, 27, 109–113.
 - [27] Zou, C. W.; Wu, H. Z.; Liang, F.; Xue, S. W.; Shao, L. X. Appl. Phys. Lett. 2014, 104, 222105.
 - [28] Wang, J. W.; Chen, Y. X.; Shi, Y. Nucl. Instrum. Methods Phys. Res., Sect. B 2013, 307, 391–393.
 - [29] Taguchi, H.; Matsu-ura, S. I.; Nagao, M.; Choso, T.; Tabata, K. J. Solid State Chem. 1997, 129, 60–65.
 - [30] Chandradass, J.; Bae, D. S.; Kim, K. H. Adv. Powder Technol. 2011, 22, 370–374.